Diabetes, Metabolic Syndrome and Obesity

Dovepress
Taylor & Francis Group

Open Access Full Text Article

ORIGINAL RESEARCH

Research on the Relationship Between Ectopic Fat and Iron Deposition in the Liver and Pancreas, with Glucose Metabolism in Elderly Obese Patients

Hao Nie[1], Min Liu[2], Junhong Duan[3], Hong Liu[2]

[1]Department of Geriatrics, Hunan Provincial People's Hospital, The First Affiliated Hospital of Hunan Normal University, Changsha, Hunan, People's Republic of China; [2]Department of Nutrition, the Third Xiangya Hospital of Central South University, Changsha, Hunan, People's Republic of China; [3]Department of Radiology, the Third Xiangya Hospital of Central South University, Changsha, Hunan, People's Republic of China

Correspondence: Hong Liu, Department of Nutrition, the Third Xiangya Hospital, Central South University, 138 Tongzipo Street, Changsha, Hunan, 410013, People's Republic of China, Email liuhong04170332@126.com

Purpose: This study investigates the clinical significance of ectopic fat and iron deposition in the liver and pancreas for glucose metabolism in elderly obese patients, with a focus on their potential for early diabetes screening and intervention.

Methods: We conducted a cross-sectional study of 140 elderly obese patients (aged 65–80 years, BMI ≥28 kg/m²) who underwent MRI quantification of hepatic and pancreatic fat (MRI-PDFF) and iron content (R2* values), along with measurements of visceral and subcutaneous fat via T2-weighted imaging. Glucose metabolism was assessed through oral glucose tolerance testing and related biomarkers.

Results: Compared to normal glucose tolerance (NGT) and impaired glucose regulation (IGR) groups, elderly obese patients with type 2 diabetes mellitus (T2DM) showed significantly higher ectopic fat in the liver (16.6% vs 6.9–13.4%) and pancreas (13.5% vs 8.5–9.0%), as well as increased visceral fat area (198.0cm² vs 137.8–163.9cm²). Liver fat percentage >11.8% was identified as an independent risk factor for abnormal glucose metabolism (*OR*=2.05, 95% *CI* 1.22–3.14), with a 2.05-fold increased risk compared to lower levels. The optimal diagnostic thresholds were determined as 11.8% for liver fat (sensitivity 83.2%, specificity 56.1%; AUC = 0.823) and 6.9% for pancreatic fat (sensitivity 72.2%, specificity 50.2%; AUC = 0.688), highlighting their clinical utility for early risk stratification.

Conclusion: Ectopic fat deposition in the liver, particularly when exceeding 11.8%, is a significant independent risk factor for glucose metabolism abnormalities in elderly obese patients. Our findings demonstrate that MRI-based quantification of hepatic fat provides a valuable tool for early identification of diabetes risk, enabling targeted interventions to prevent disease progression. This study highlights the clinical importance of monitoring ectopic fat deposition in clinical practice for elderly obese populations.

Keywords: magnetic resonance imaging, ectopic fat deposition, iron deposition, elderly obese patients, type 2 diabetes mellitus

Introduction

The global epidemic of obesity and type 2 diabetes mellitus (T2DM) among the elderly has reached alarming proportions, presenting unprecedented challenges to healthcare systems worldwide. China alone reported over 35.5 million elderly individuals with diabetes in 2019, accounting for one-quarter of the global elderly diabetic population.[1,2] While obesity, particularly central obesity, has been firmly established as a major risk factor for insulin resistance and T2DM, conventional anthropometric measures such as body mass index (BMI) and waist circumference demonstrate significant limitations in capturing the complex metabolic disturbances associated with ectopic fat deposition. This abnormal fat accumulation in non-adipose tissues, particularly the liver and pancreas, differs fundamentally from visceral fat (defined as adipose tissue deposited within the abdominal cavity, surrounding internal organs such as the intestines and kidneys)

Received: 19 January 2025
Accepted: 8 July 2025
Published: 14 July 2025

Graphical Abstract

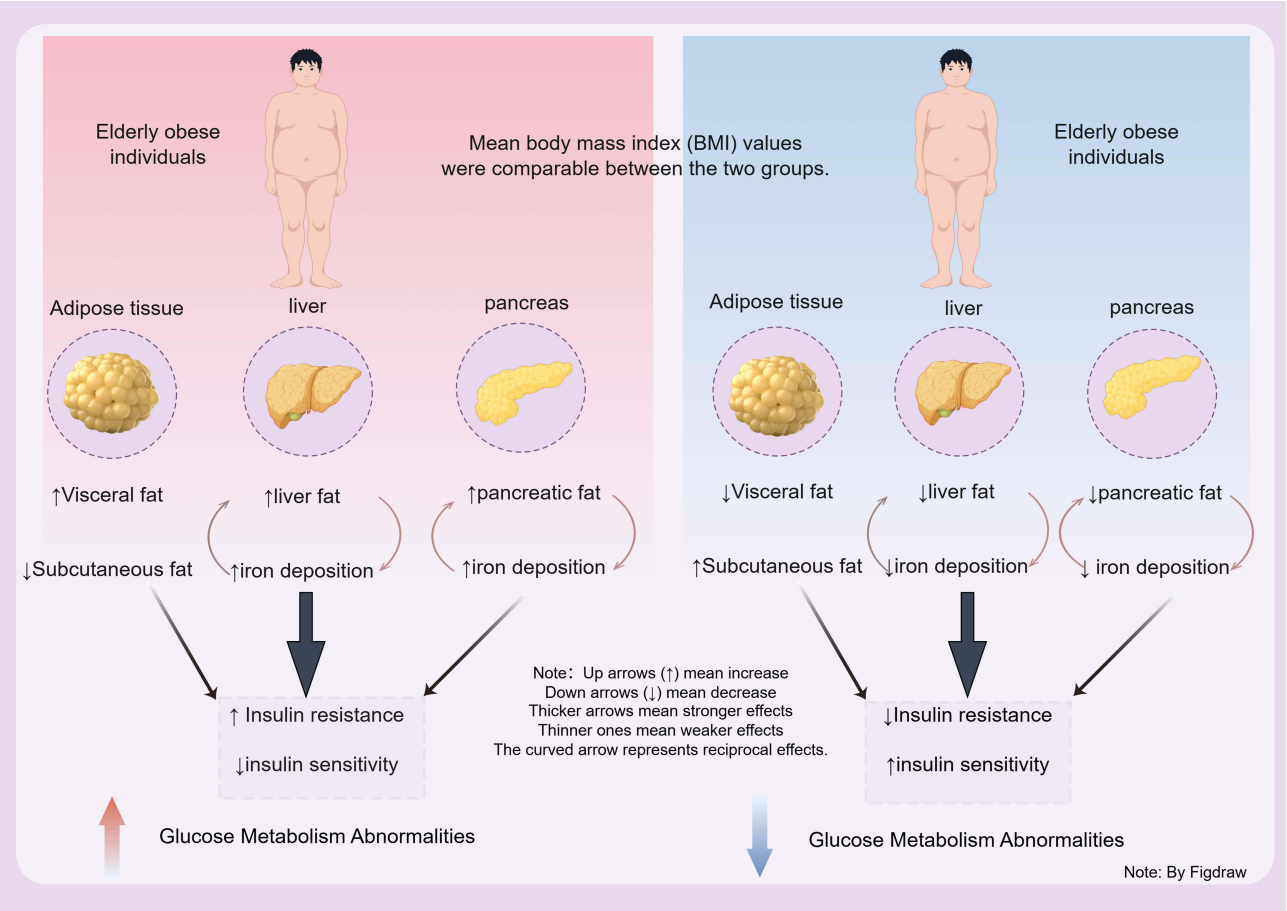

and subcutaneous fat (defined as fat stored beneath the skin). Ectopic fat deposition has emerged as a critical pathogenic factor in the development of insulin resistance and glucose metabolism abnormalities through mechanisms involving lipid overflow and lipotoxicity.

Recent advances in magnetic resonance imaging (MRI) technology have revolutionized our ability to quantify organ-specific fat content and iron deposition.[3,4] Techniques such as magnetic resonance imaging proton density fat fraction (MRI-PDFF) and R2* mapping now enable precision in assessing hepatic and pancreatic fat content and iron overload,[3,4] unlike conventional serum markers like ferritin, which are confounded by inflammation and other non-specific factors,[5,6] thereby addressing critical limitations in current diagnostic approaches for metabolic disorders. Despite accumulating evidence linking ectopic fat deposition to metabolic dysfunction, clinical practice continues to rely heavily on BMI and fasting glucose measurements for risk stratification, which demonstrate inadequate sensitivity for detecting early metabolic abnormalities, particularly in elderly populations where age-related changes in body composition complicate risk assessment, and existing imaging modalities often fail to differentiate between metabolically distinct fat depots (visceral vs subcutaneous), further underscoring the urgent need for more precise diagnostic tools.

To address these critical gaps, this study aims to: (1) investigate the relationship between ectopic fat deposition (specifically in the liver and pancreas) and iron deposition with abnormal glucose metabolism (including impaired glucose regulation and T2DM) in elderly obese patients; (2) compare the relative contributions of different fat depots, particularly visceral fat versus ectopic fat, to metabolic dysfunction; and (3) establish a more accurate risk stratification

model for early diabetes detection in high-risk populations through integrating MRI assessments with glucose metabolic profiling. By employing advanced MRI techniques to quantify organ-specific fat and iron deposition, our study hypothesizes that organ-specific fat accumulation, when exceeding defined thresholds, serves as an independent risk factor for glucose metabolism abnormalities, offering superior predictive value compared to traditional markers. The novelty of our research approach lies in its simultaneous assessment of both fat and iron deposition in metabolically active organs, providing a more comprehensive understanding of the pathophysiological mechanisms underlying glucose dysregulation, while its focus on elderly obese patients - an understudied yet high-risk population - addresses a critical gap in current research and offers potential implications for personalized diabetes prevention strategies. The findings from this investigation could ultimately inform clinical guidelines regarding the implementation of MRI-based biomarkers for early intervention and risk management in geriatric metabolic disorders.

Materials and Methods

Study Subjects

This study is a cross-sectional research. Elderly obese patients who visited the Nutrition Department of the Xiangya Hospital of Central South University from Oct 2022 to Aug 2024 were prospectively recruited. Inclusion criteria: (1) Age between 65 and 80 years; (2) Body mass index (BMI)≥28 kg/m²; (3) Ability to cooperate with various examinations. Exclusion criteria: (1) Patients with a prior confirmed diagnosis of diabetes who have already started medication; (2) Patients with malignant tumors; (3) Acute infections; (4) Hemochromatosis; (5) Chronic inflammatory diseases; (6) Concurrent hepatitis; (7) Unexplained elevation of liver enzymes; (8) Iron-deficiency anemia with iron supplementation; (9) Blood donors or transfusion recipients within the past 6 months; (10) History of cardiovascular events within the past 6 months; (11) Acute or chronic blood loss; (12) Excessive alcohol consumption (males with weekly alcohol intake >140 grams, females >70 grams); (13) Use of medications affecting weight or weight fluctuation ≥5% in the past 3 months.

Research Methods

General Data Collection

Data were collected on patients' age, sex, height, weight, waist circumference, hip circumference, details of physical activity and medication information.

Biochemical Indicators

All patients underwent oral glucose tolerance test (OGTT). Fasting venous blood samples were collected, and biochemical indicators such as liver and kidney function tests and blood lipids were measured using a fully automated biochemical analyzer (Hitachi 7600, Japan). Serum ferritin was determined using chemiluminescent microparticle immunoassay (CMIA) technology. Blood glucose and glycosylated hemoglobin were measured using the enzyme electrode method (Aikola GA-1172, Japan), and insulin was measured using electrochemiluminescence (Roche 601, Germany).

Calculation Formulas

The insulin resistance index (HOMA-IR) was calculated as: HOMA-IR = (fasting plasma glucose × fasting insulin) / 22.5 and beta-cell function (HOMA-β) was calculated as: HOMA-β= 20 × fasting insulin / (fasting plasma glucose - 3.5).[7] The insulin sensitivity was calculated using the insulin sensitivity index (ISI), which is calculated as: ISI = 10,000 / √(fasting plasma glucose × fasting insulin × 2-hour postload glucose × 2-hour postload insulin).[7] Units for FPG are mmol/L and for FINS are μU/mL. The triglyceride index (TyG) was calculated as: TyG = Ln[(fasting triglycerides (mg/dL) × fasting plasma glucose (mg/dL)) / 2].[7]

Assessment of Dietary Intake

Usual food and nutrient intake was estimated based on repeated 24-h food lists (24H-FL). Up to three 24H-FL per participant were used to assess the foods consumed on the previous day and consisted of 246 food items. Energy and

nutrient intakes were estimated by means of the China food composition table The present analysis includes macronutrients (carbohydrates, protein, fat) as well as related subcategories (fiber) and selected micronutrients (iron).

Magnetic Resonance Imaging (MRI)

All patients underwent MRI examinations performed by a professional radiologist with 8 years of experience, in a fasting state, utilizing the MRI imaging system (INGENIA ELITION X, Philips Medical System, Nederland) and multi-echo Dixon sequence technology. Eight 100 mm² regions of interest (ROI) were selected in the right lobe of the liver to obtain the average liver fat content (liver MRI-PDFF, %) and liver iron content (liver MRI-R2*sec^{-1}); for the head, body, and tail of the pancreas, a 100 mm² ROI was selected and averaged to obtain pancreatic fat content (pancreatic MRI-PDFF, %) and pancreatic iron content (pancreatic MRI-R2*sec^{-1}). Using Slice O matic software, subcutaneous and visceral fat at the level of the L3 vertebra's transverse process from T2-weighted imaging sequence were outlined to obtain the corresponding areas (cm²).

Statistical Analysis

All results were statistically processed using R software (version 3.5.3) and SPSS 24.0. Count data were expressed as rates (%), while measurement data were represented as mean ± standard deviation or median (*Q1, Q3*). *ANOVA* or Kruskal–Wallis *H*-test was used for comparing differences in means among three groups. Pairwise comparisons among three groups were conducted using post-hoc Bonferroni correction. The correlation between serological indicators and imaging results was analyzed using Pearson or Spearman correlation analysis. Receiver operating characteristic (ROC) curves were plotted for liver and pancreatic fat content and iron deposition regarding abnormal glucose metabolism. Logistic regression analyzed the relationship between ectopic fat deposition and abnormal glucose metabolism: variables with a *P*-value <0.1 from univariate regression entered multivariate regression models. A $P < 0.05$ was considered statistically significant.

Results

Baseline Characteristics

A total of 140 elderly obese patients were included in this study. Based on the OGTT results, they were divided into three groups: 46 cases of T2DM, 44 cases of impaired glucose regulation (IGR), and 50 cases with normal glucose tolerance (NGT). No statistically significant differences among the three groups in terms of total energy, protein, fat, cholesterol, fiber, and iron intake, as well as physical activity levels and medication use. T2DM group showed significantly higher carbohydrate intake than NGT/IGR groups (Supplementary Table 1).

Clinical Parameters: Glucose metabolism deterioration from NGT to T2DM was marked by rising fasting, 0.5h/2h post-OGTT glucose, and HOMA-IR, alongside elevated triglycerides/cholesterol, reduced HOMA-β/ISI, and increased serum ferritin vs NGT/IGR (Table 1, Supplementary Table 2).

MRI: Glucose metabolism deterioration from NGT to T2DM showed progressive increases in visceral, hepatic, and pancreatic fat/iron deposition, with decreasing subcutaneous fat. The T2DM group exhibited significantly higher hepatic/pancreatic fat/iron than NGT (Table 2, Supplementary Table 3 and Figure 1).

ROC Analysis for Predictive Performance

Hepatic ectopic fat deposition showed excellent predictive ability for glucose metabolism abnormalities (*AUC*=0.823, 95% *CI*: 0.705–0.940, *P*<0.05), with optimal cutoff at 11.8% fat content (sensitivity=83.2%, specificity=56.1%).

Pancreatic ectopic fat deposition showed moderate predictive value (*AUC*=0.688, 95% *CI*: 0.532–0.845, *P*<0.05), with optimal cutoff at 6.9% fat content (sensitivity=72.2%, specificity=50.2%) (Figure 2A).

For iron deposition markers: Liver MRI-R2* demonstrated good predictive performance (*AUC*=0.756, 95% *CI*: 0.607–0.905, *P*<0.05), with optimal cutoff at 49.9 s^{-1} (sensitivity=70.8%, specificity=47.7%). Pancreatic MRI-R2* showed fair predictive value (*AUC*=0.663, 95% *CI*: 0.504–0.822, *P*<0.05), with optimal cutoff at 31.3 s^{-1} (sensitivity=64.0%, specificity=40.2%) (Figure 2B).

Table 1 Comparison of Clinical Characteristics Among Elderly Obese Patients with Different Glucose Metabolism States

	Normal Glucose Tolerance (n=50)	Impaired Glucose Regulation (n=44)	Type 2 Diabetes Mellitus (n=46)	*P* value
Gender (Male)	26 (52.0)	24 (54.5)	23 (50.0)	0.911
Age, years	68.2 (65.3, 72.2)	68.3 (65.8, 71.1)	68.5 (65.8, 71.8)	0.092
BMI, kg/m2	29.2 (28.0, 31.3)	29.4 (28.2, 32.0)	29.8 (28.0, 32.5)	0.152
Waist-to-hip ratio	0.97±0.12	0.97±0.04	0.99±0.26	0.195
Hypertension	12 (24.0)	8 (18.2)	15 (32.6)	0.281
Triglycerides, mmol/L	2.0 (1.1, 2.9)	2.7 (2.0, 4.5)	3.2 (2.5, 4.9)	0.007**
TC, mmol/L	4.9 (3.3, 6.0)	4.9 (3.9, 6.2)	6.0 (5.1, 7.6)	0.040*
Ferritin, μg/L	96.4 (63.9, 182.0)	122.5 (78.4, 256.0)	289.0 (185.6, 498.5)	<0.001***
Triglyceride index	3.9±0.7	4.2 ±0.7	4.8±1.3	<0.001***
Fasting blood glucose, mmol/L	5.3 (4.5, 5.9)	5.8 (5.6, 7.0)	9.8 (7.9, 13.5)	<0.001***
OGTT-0.5 h, mmol/L	8.8 (8.0, 9.7)	10.0 (9.0, 11.0)	15.7 (12.0, 18.3)	<0.001***
OGTT-2 h, mmol/L	6.6 (5.2, 7.1)	9.8 (8.2, 10.5)	18.8 (14.9, 21.4)	<0.001***
HOMA-IR	4.5 (3.6, 5.7)	4.8 (3.8, 8.4)	6.6 (4.2, 10.4)	0.005**
HOMA-β, %	242.3 (187.4, 346.2)	184.2 (136.7, 274.2)	69.2 (33.0, 92.3)	<0.001***
ISI	46.6 (30.1, 64.0)	26.6 (16.7, 44.1)	21.2 (10.1, 31.2)	<0.001***

Notes: Normal distribution is expressed as: Mean±Standard Deviation; Skewed distribution is expressed as: Median (*Q1, Q3*); Count data were expressed as rates (%). **P*<0.05, ***P*<0.01, ****P*<0.001.

Abbreviations: BMI, body mass index; TC, Total Cholesterol; HOMA-IR, Homeostasis Model Assessment of Insulin Resistance; HOMA-β, Homeostasis Model Assessment of Beta Cell Function; ISI, Insulin Sensitivity Index.

Table 2 Comparison of Ectopic Fat and Iron Deposition Among Elderly Obese Patients with Different Glucose Metabolism States

	NGT	IGR	T2DM	*P* value
Subcutaneous fat area, cm2	278.8 (200.1, 335.6)	232.9 (180.3, 330.4)	171.2 (115.2, 225.0)	<0.001***
Visceral fat area, cm2	137.8 (90.3, 165.5)	163.9 (99.2, 199.8)	198.0 (158.8, 359.4)	0.01*
Liver fat percentage, %	6.9 (5.8, 13.9)	13.4 (9.2, 22.8)	16.6 (12.6, 33.8)	0.008**
Liver iron, sec-1	46.6 (39.8, 59.2)	58.1 (47.5, 63.3)	65.6 (52.3, 67.2)	0.01*
Pancreatic fat percentage, %	8.5 (5.7, 11.2)	9.0 (5.9, 19.1)	13.5 (6.9, 29.0)	<0.001***
Pancreatic iron, sec-1	27.2 (24.0, 35.3)	29.2 (23.0, 38.9)	34.4 (28.4, 39.6)	<0.001***

Notes: Skewed distribution is expressed as: Median (*Q1, Q3*). **P*<0.05, ***P*<0.01, ****P*<0.001.

Abbreviations: NGT, Normal Glucose Tolerance; IGR, Impaired Glucose Regulation; T2DM, Type 2 Diabetes Mellitus.

Logistic Regression Confirming Independent Predictive Role

Multivariate logistic regression revealed that both hepatic fat percentage >11.8% (*OR*=2.05, 95% *CI*: 1.22–3.14, *P*=0.035) and subcutaneous fat area <287.5 cm² (*OR*=1.80, 95% *CI*: 1.44–4.85, *P*=0.006) independently predicted increased risk of abnormal glucose metabolism in elderly obese patients (Table 3).

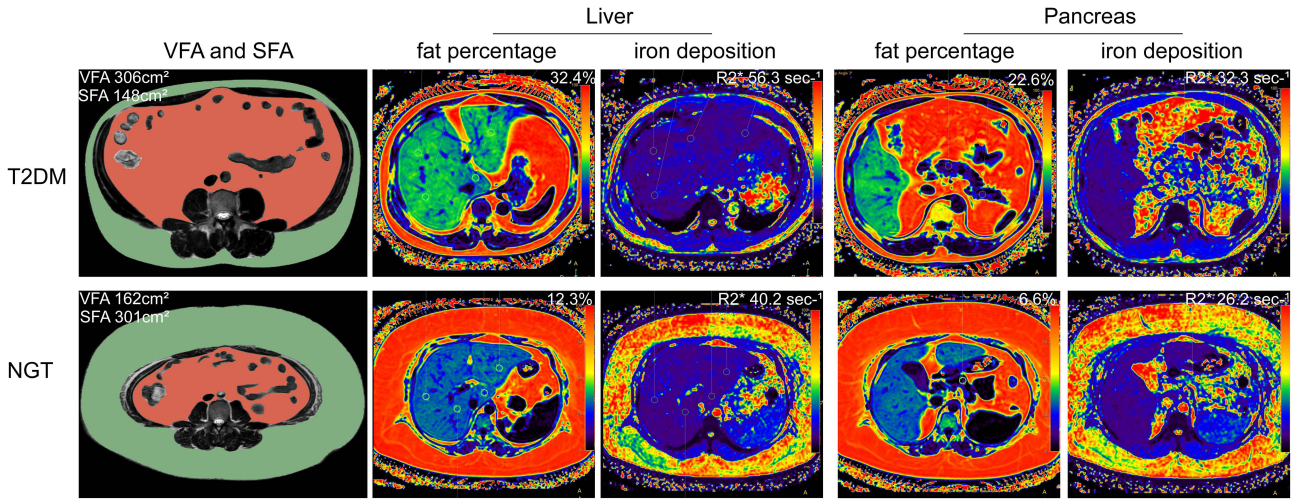

Figure 1 MRI images of visceral and subcutaneous fat areas, as well as liver and pancreatic fat content and iron deposition in elderly obese patients with normal glucose tolerance and type 2 diabetes.
Note: normal glucose tolerance (NGT) patient (68 years old, male, BMI=30.6 kg/m²); type 2 diabetes mellitus (T2DM) patient (68 years old, male, BMI=30.5 kg/m²).

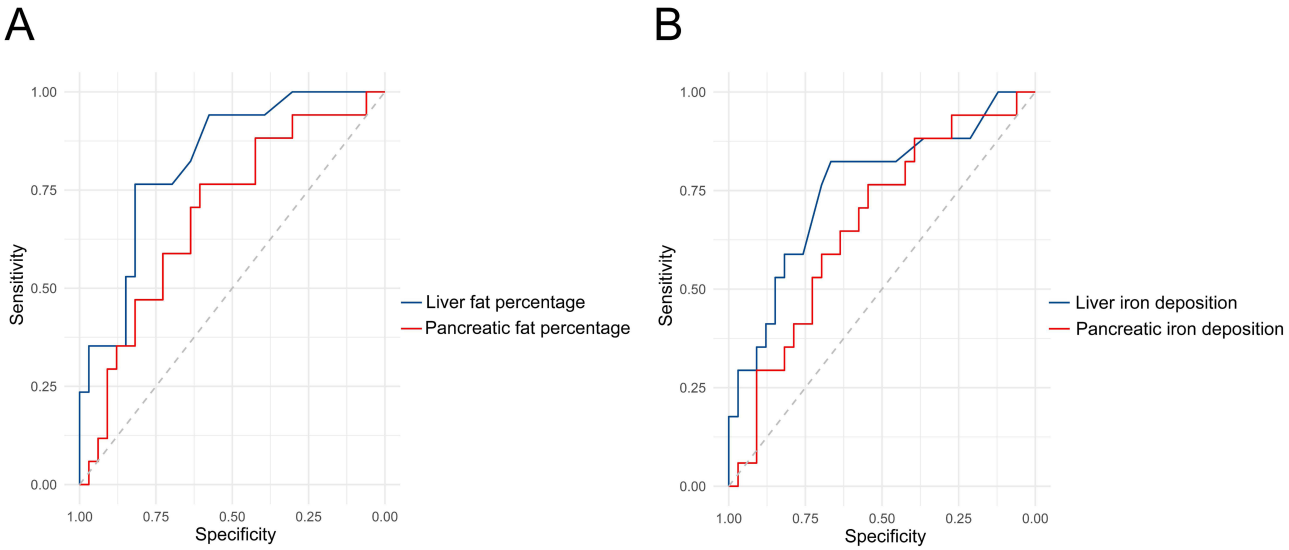

Figure 2 Area Under the ROC Curve for Predicting Glucose Metabolism Abnormalities (IGR and T2DM) in Elderly Obese Patients Using MRI-Detected Ectopic Fat and Iron Deposition. (**A**) Area under the ROC curve for predicting glucose metabolism abnormalities based on MRI-detected liver and pancreatic fat; (**B**) Area under the ROC curve for predicting glucose metabolism abnormalities based on MRI-detected liver and pancreatic iron deposition.
Abbreviations: IGR, Impaired Glucose Regulation; T2DM, Type 2 Diabetes Mellitus.

Notably, when using the clinically established cutoff of 10% for hepatic fat (≥10% indicating moderate/severe fatty liver), the results remained robust (*OR*=1.90, 95% *CI*: 1.14–3.21, *P*=0.040) (Supplementary Table 4).

Correlation Analyses

Correlation analyses uncovered several significant relationships. In terms of ectopic fat - glucose metabolism, liver MRI - PDFF was positively correlated with HOMA - IR ($r = 0.59$, $P < 0.001$) and OGTT glucose at all timepoints ($P \leq 0.002$), while negatively correlated with ISI ($r = -0.44$, $P < 0.05$). Pancreatic MRI - PDFF was negatively correlated with HOMA - β ($r = -0.327$, $P = 0.0001$) and positively correlated with OGTT glucose at all timepoints ($P \leq 0.002$).

Regarding iron deposition - glucose metabolism, liver MRI - R2* was positively correlated with HOMA - IR ($r = 0.31$, $P = 0.002$) and OGTT glucose at all timepoints ($P < 0.001$), and negatively correlated with ISI ($r = -0.32$, $P < 0.001$).

Table 3 Logistic Regression Analysis of the Relationship Between Ectopic Fat and Iron Deposition, and Glucose Metabolism Abnormalities in Elderly Obese Patients

	Univariate Regression		Multivariate Regression	
	OR (95% *CI*)	***P***	**OR (95% *CI*)**	***P***
Age	3.83 (0.88–8.80)	0.212		
Gender	0.80 (0.47–1.23)	0.370		
Body mass index	0.52 (0.40–1.42)	0.621		
Physical activity	0.62 (0.35–1.40)	0.320		
Medication use	0.89 (0.22–5.73)	0.650		
Total energy intake	1.23 (0.87–1.69)	0.165		
Fat intake	1.12 (0.54–1.51)	0.185		
Carbohydrates intake	1.42 (0.83–2.45)	0.082*	1.20 (0.69–1.44)	0.138
Ferritin	3.80 (1.90–6.94)	0.01**	2.12 (0.75–4.80)	0.082
Liver fat percentage	4.29 (2.04–7.20)	0.001***	2.05 (1.22–3.14)	0.035**
Liver iron deposition	4.27 (2.16–7.85)	0.01**	2.29 (0.84–5.57)	0.128
Pancreatic fat percentage	1.74 (1.02–3.70)	0.030**	0.94 (0.50–2.17)	0.751
Pancreatic iron deposition	1.78 (0.88–3.29)	0.085*	1.17 (0.35–2.25)	0.351
Visceral fat area	3.66 (1.50–9.67)	0.030**	1.51 (0.67–5.18)	0.241
Subcutaneous fat area	4.80 (2.48–7.97)	0.005***	1.80 (1.44–4.85)	0.006***

Notes: Dependent variable: Normal glucose metabolism = 0; Abnormal glucose metabolism = 1 (including impaired glucose tolerance and type 2 diabetes mellitus). Independent variables: Gender, Female = 0, Male = 1; Age, < 68.0 years = 0, ≥ 68.0 years = 1; Physical activity, no activity or sporadically=0, regularly more than 1h/week =1; Medication use, no=0, yes=1; Total energy intake, <1850kcal=0, ≥ 1850kcal=1; Fat, <78.0g=0, ≥ 78.0g=1; Carbohydrates, <280g=0, ≥ 280g=1; Body Mass Index, < 29.0 kg/m² = 0, ≥ 29.0 kg/m² = 1; Ferritin, < 184.5 μg/L = 0, ≥ 184.5 μg/L = 1; Liver fat percentage, < 11.8% = 0, ≥ 11.8% = 1; Pancreatic fat percentage, < 6.9% = 0, ≥ 6.9% = 1; Liver iron deposition, < 49.9 s^{-1} = 0, ≥ 49.9 s^{-1} = 1; Pancreatic iron deposition, < 31.3 s^{-1} = 0, ≥ 31.3 s^{-1} = 1; Visceral fat area, < 128.0 cm² = 0, ≥ 128.0 cm² = 1; Subcutaneous fat area, ≥ 287.5 cm² = 0, < 287.5 cm² = 1; * *P*<0.10, ** *P*<0.05, *** *P*<0.01.

Abbreviation: OR(95% *CI*), Odds Ratio (95% Confidence Interval).

Pancreatic MRI - R2* was negatively correlated with HOMA - β (r = - 0.287, P = 0.001) and positively correlated with OGTT glucose at all timepoints ($P \leq 0.006$).

In the aspect of fat - iron deposition, there was a strong positive correlation between MRI - PDFF and MRI - R2*showing a significant positive correlation between liver MRI-PDFF and liver MRI-R2* (r=0.77, P<0.001), as well as between pancreatic MRI-PDFF and pancreatic MRI-R2* (r=0.70, P=0). For iron biomarker validation, both liver MRI - R2* and pancreatic MRI - R2* were strongly positively correlated with serum ferritin (r = 0.69 and 0.45, respectively, P < 0.001).

Discussion

This study identifies hepatic and pancreatic ectopic fat deposition as predictors of abnormal glucose metabolism (including IGR and T2DM) in elderly obese patients, with hepatic fat demonstrating superior predictive value. These findings carry significant clinical implications for early screening and targeted interventions, particularly through the lens of altered adipose tissue distribution and fat redistribution between storage compartments.

Clinical Implications and Early Screening

MRI-derived hepatic fat percentage >11.8% was an independent predictor of glucose metabolism abnormalities (*OR*=2.05, 95% *CI*: 1.22–3.14, *P*=0.035), while subcutaneous fat area <287.5 cm² was an independent risk factor (*OR*=1.80, 95% *CI*: 1.44–4.85, *P*=0.006). These thresholds enable non-invasive risk stratification, facilitating early intervention before β-cell dysfunction develops. The clinical significance of these findings lies in their ability to identify high-risk individuals through readily available imaging modalities. Notably, the association between reduced subcutaneous fat area and increased diabetes risk highlights the importance of adipose tissue distribution patterns, where a smaller subcutaneous fat depot may reflect impaired capacity for healthy fat storage, leading to ectopic fat deposition in more metabolically active organs like the liver. This concept of fat redistribution from protective subcutaneous compartments to harmful visceral and ectopic sites provides a mechanistic framework for understanding the observed associations.

Pathogenic Role of Ectopic Fat Deposition

Hepatic fat deposition showed stronger associations with glucose metabolism than pancreatic fat or visceral fat. Liver fat percentage >11.8% increased diabetes risk by 2.05-fold, consistent with meta-analyses linking MAFLD to T2DM (HR=1.97, 95% CI: 1.80–2.15) and prospective studies showing 58% T2DM incidence in MAFLD patients within 5 years.[8,9] This pronounced association underscores the liver's central role in glucose metabolism and its particular vulnerability to fat accumulation in the context of obesity.[10,11] Pancreatic fat, while correlated with β-cell dysfunction in univariate analysis, lost significance after adjusting for liver fat (*P*=0.751), suggesting its role is secondary to hepatic fat deposition.[12–15] This hierarchical relationship among different fat depots emphasizes the primacy of hepatic fat accumulation in disrupting metabolic homeostasis. The pattern of fat redistribution we observed, characterized by increased hepatic fat deposition and decreased subcutaneous fat area, aligns with the concept of pathological fat redistribution away from protective storage sites toward metabolically harmful locations.

Therapeutic Implications: Liver-First Approach and Iron Modulation

The liver's central role in glucose metabolism dysfunction supports prioritizing liver-targeted interventions (eg, lifestyle modifications, pioglitazone) to reduce hepatic fat and improve insulin sensitivity.[10,11] Elevated liver/pancreas MRI-R2* (iron deposition markers) correlated with insulin resistance and predicted glucose abnormalities (AUC=0.756–0.663). Given iron overload's documented role in β-cell toxicity, therapies modulating iron homeostasis (eg, phlebotomy, iron chelators) may warrant investigation.[16–19] The preferential accumulation of fat in the liver and associated iron deposition create a particularly detrimental metabolic environment that could be specifically targeted for intervention. This liver-first approach is supported by our finding that hepatic fat percentage was the most robust predictor of abnormal glucose metabolism among all evaluated fat depots.

Pancreatic Fat: Driver or Consequence?

Pancreatic fat's association with glucose abnormalities diminished after adjusting for liver fat (P=0.751), supporting the hypothesis that pancreatic fat reflects systemic metabolic dysregulation rather than directly driving β-cell dysfunction.[12–15] This finding reinforces the concept that pancreatic fat deposition is more likely a consequence of systemic metabolic disturbances, particularly hepatic fat accumulation, rather than a primary driver of β-cell dysfunction. The secondary role of pancreatic fat underscores the importance of addressing hepatic fat deposition as the primary therapeutic target.

Iron Overload and Diabetes Pathogenesis

Elevated serum ferritin and organ iron deposition (liver/pancreas R2*) correlated with insulin resistance and glucose abnormalities. Liver iron deposition was linked to increased liver fat content, while pancreatic iron deposition correlated with pancreatic fat. These findings align with studies showing iron overload induces oxidative stress, steatosis, and β-cell dysfunction, providing mechanistic plausibility for its role in diabetes pathogenesis.[16–19] The association between iron deposition and metabolic dysfunction further supports the concept of a detrimental adipose tissue redistribution pattern,

where increased iron accumulation in metabolically active organs exacerbates the metabolic consequences of fat misallocation.

Fat Redistribution and Adipose Tissue Dysfunction

An emerging concept from our findings is the critical role of altered adipose tissue distribution in the pathogenesis of abnormal glucose metabolism. The significant association between reduced subcutaneous fat area (<287.5 cm^2) and increased diabetes risk highlights the loss of protective fat storage capacity, forcing excess fat to accumulate in more metabolically harmful locations such as the liver. This fat redistribution pattern, characterized by decreased subcutaneous fat and increased hepatic fat deposition, creates a metabolically precarious state that predisposes to insulin resistance and β-cell dysfunction. The concept of adipose tissue dysfunction extending beyond simple fat quantity to include fat distribution patterns provides a more nuanced understanding of metabolic disease pathogenesis and offers new avenues for risk stratification and intervention.

Limitations and Future Directions

As a cross-sectional study, causality remains inferred. Longitudinal trials are required to validate MRI biomarkers' predictive durability and therapeutic impact. Mechanistic studies should clarify pancreatic fat's role in diabetes progression. Future research should focus on elucidating the mechanisms underlying fat redistribution and its metabolic consequences, as well as evaluating interventions targeting this pathological process. Additionally, studies investigating the potential benefits of strategies to restore healthy fat distribution patterns, such as interventions promoting subcutaneous fat expansion or reducing hepatic fat accumulation, could provide valuable insights for clinical management.

Conclusion

These findings reveal that fat redistribution from protective subcutaneous depots to harmful visceral/ectopic sites drives metabolic dysfunction. MRI-derived thresholds (hepatic fat >11.8%, subcutaneous fat <287.5 cm^2) enable early risk stratification before β-cell dysfunction becomes irreversible, highlighting the need for prospective biomarker validation, interventions targeting hepatic fat/iron modulation, and mechanistic studies to inform therapeutic strategies for high-risk elderly populations.

Data Sharing Statement

The data supporting the findings of this study are available within the article and its supplementary materials.

Ethics Approval and Informed Consent

This study complies with the Declaration of Helsinki. All study subjects signed an informed consent form. This study has been approved by the Ethics Committee of the third Xiangya Hospital of Central South University (approval number: I 22218).

Consent for Publication

We affirm that the specifics of any images, videos, recordings, etc., are authorized for publication, and the individuals granting consent have been informed about the content of the article that will be published. We are willing to provide copies of signed consent forms to the journal's editorial office if needed.

Acknowledgments

We would like to thank our colleagues in the department for their guidance and strong support during this research and paper writing process.

Author Contributions

All authors made a significant contribution to the work reported, whether that is in the conception, study design, execution, acquisition of data, analysis and interpretation, or in all these areas; took part in drafting, revising or critically reviewing the article; gave final approval of the version to be published; have agreed on the journal to which the article has been submitted; and agree to be accountable for all aspects of the work.

Funding

The Natural Science Foundation of Hunan Province, China (2022JJ40749); Scientific Research Project of Hunan Provincial Health Commission, China (202203065334); Scientific Research Project of Hunan Provincial Health Care Special Fund,China (B2022-01).;

Disclosure

The author(s) report no conflicts of interest in this work.

References

1. NCD Risk Factor Collaboration (NCD-RisC). Worldwide trends in underweight and obesity from 1990 to 2022: a pooled analysis of 3663 population-representative studies with 222 million children, adolescents, and adults. *Lancet*. 2024;403(10431):1027–1050. doi:10.1016/S0140-6736(23)02750-2
2. Chen K, Shen ZW, Gu WJ, et al. Prevalence of obesity and associated complications in China: A cross-sectional, real-world study in 15.8 million adults. *Diabetes Obes Metab*. 2023;25(11):3390–3399. doi:10.1111/dom.15238
3. Kim JW, Lee CH, Yang Z, et al. The spectrum of magnetic resonance imaging proton density fat fraction (MRI-PDFF), magnetic resonance spectroscopy (MRS), and two different histopathologic methods (artificial intelligence vs. pathologist) in quantifying hepatic steatosis. *Quant Imaging Med Surg*. 2022;12(11):5251–5262. doi:10.21037/qims-22-393
4. Grimm A, Meyer H, Nickel MD, et al. Repeatability of Dixon magnetic resonance imaging and magnetic resonance spectroscopy for quantitative muscle fat assessments in the thigh. *J Cachexia, Sarcopenia Muscle*. 2018;9(6):1093–1100. doi:10.1002/jcsm.12343
5. Gao H, Yang JY, Pan WF, et al. Iron overload and the risk of diabetes in the general population: results of the Chinese health and nutrition survey cohort study. *Diabetes Metab J*. 2022;46(2):307–318. doi:10.4093/dmj.2020.0287
6. Liu JF, Li QX, Yang YX, et al. Iron metabolism and type 2 diabetes mellitus: a meta-analysis and systematic review. *J Diabetes Investig*. 2020;11(4):946–955. doi:10.1111/jdi.13216
7. Liu MM, Liu QJ, Wen J, et al. Waist-to-hip ratio is the most relevant obesity index at each phase of insulin secretion among obese patients. *J Diabetes Complications*. 2018;32(7):670–676. doi:10.1016/j.jdiacomp.2018.04.006
8. Ballestri S, Zona S, Targher G, et al. Nonalcoholic fatty liver disease is associated with an almost twofold increased risk of incident type 2 diabetes and metabolic syndrome. Evidence from a systematic review and meta-analysis. *J Gastroenterol Hepatol*. 2016;31(5):936–944. doi:10.1111/jgh.13264
9. Ekstedt M, Franz´en LE, Mathiesen UL, et al. Long-term follow-up of patients with NAFLD and elevated liver enzymes. *Hepatol*. 2006;44(4):865–873. doi:10.1002/hep.21327
10. Fukuda T, Hamaguchi M, Kojima T, et al. Transient remission of nonalcoholic fatty liver disease decreases the risk of incident type 2 diabetes mellitus in Japanese men. *Eur J Gastroenterol Hepatol*. 2016;28(12):1443–1449. doi:10.1097/MEG.0000000000000736
11. Mrabeh AA, Zhyzhneuskaya SV, Peters C, et al. Hepatic lipoprotein export and remission of human type 2 diabetes after weight loss. *Cell Metab*. 2020;31(2):233–249. doi:10.1016/j.cmet.2019.11.018
12. Wu WJ. Diabetes remission and nonalcoholic fatty pancreas disease. *World J Diabetes*. 2024;15(7):1390–1393. doi:10.4239/wjd.v15.i7.1390
13. Wagner R, Eckstein SS, Yamazaki H, et al. Metabolic implications of pancreatic fat accumulation.*Nat*. *Rev Endocrino*. 2022;18(1):43–54. doi:10.1038/s41574-021-00573-3
14. Heni M, Machann J, Staiger H, et al. Pancreatic fat is negatively associated with insulin secretion in individuals with impaired fasting glucose and/or impaired glucose tolerance: a nuclear magnetic resonance study. *Diabetes Metab Res Rev*. 2010;26(3):200–205. doi:10.1002/dmrr.1073
15. Chan TT, Tse YK, Lui RNS, et al. Fatty pancreas is independently associated with subsequent diabetes mellitus development: a 10-year prospective cohort study. *Clin Gastroenterol Hepatol*. 2022;20(9):2014–2022. doi:10.1016/j.cgh.2021.09.027
16. O'Brien J, Powell LW. Non-alcoholic fatty liver disease: is iron relevant? *Hepatol Int*. 2012;6(1):332–341. doi:10.1007/s12072-011-9304-9
17. Valenzuela R, Rincón-Cervera MÁ, Echeverría F, et al. Iron-induced pro-oxidant and pro-lipogenic responses in relation to impaired synthesis and accretion of long-chain polyunsaturated fatty acids in rat hepatic and extrahepatic tissues. *Nutrition*. 2018;45:49–58. doi:10.1016/j.nut.2017.07.007
18. Yu LL, Yan JY, Zhang Q, et al. Association between serum ferritin and blood lipids: influence of diabetes and hs-CRP Levels. *J Diabetes Res*. 2020;2020:1–12. doi:10.1155/2020/4138696
19. Jahng JWS, Alsaadi RM, Palanivel R, et al. Iron overload inhibits late stage autophagic flux leading to insulin resistance. *EMBO Rep*. 2019;20(10). doi:10.15252/embr.201947911